Journal of Ginseng Research 48 (2024) 592–602

Contents lists available at ScienceDirect

Journal of Ginseng Research

journal homepage: www.sciencedirect.com/journal/journal-of-ginseng-research

Research Article

Panax notoginseng saponins promotes angiogenesis after cerebral ischemia-reperfusion injury

Haiyan Xiao [a,b,c], Shusen Liu [a,b,c,f], Binyu Fang [a,b,c,f], Wenchao Zhang [a,b,c], Min Wang [a,b,c], Jingxue Ye [a,b,c], Tianxiao Huang [e], Li Cao [a,b,c,*], Xiaojun Zhang [d,**], Guibo Sun [a,b,c,***]

[a] Beijing Key Laboratory of Innovative Drug Discovery of Traditional Chinese Medicine (Natural Medicine) and Translational Medicine, Institute of Medicinal Plant Development, Chinese Academy of Medical Sciences & Peking Union Medical College, Beijing, China
[b] Key Laboratory of New Drug Discovery Based on Classic Chinese Medicine Prescription , Chinese Academy of Medical Sciences, Beijing, China
[c] State Key Laboratory for Quality Ensurance and Sustainable Use of Dao-di Herbs, Beijing, China
[d] Xiyuan Hospital, China Academy of Chinese Medical Sciences, Beijing, China
[e] College of Life Sciences, Wuhan University, Wuhan, China
[f] Harbin University of Commerce, Harbin, Heilongjiang, China

ARTICLE INFO

Keywords:
Xueshuantong injection
Cerebral ischemic stroke
Angiogenesis
VEGF
HIF1-α

ABSTRACT

Background: Ischemic stroke is a devastating disease that can result in permanent disability and death, and angiogenesis plays a critical role in the recovery and survival of patients and animal models of ischemic stroke. Panax notoginseng has been used as a key herb in the treatment of stroke diseases due to its effect in promoting blood circulation and removing blood stasis. However, the role of Panax notoginseng saponins, in promoting angiogenesis is unclear.

Purpose: This study is aimed to investigate the effect of Xueshuantong (XST) injection, composed of Panax notoginseng saponins in post-stroke revascularization.

Method: In the present study, a middle cerebral artery occlusion/reperfusion model was established in Sprague-Dawley rats, with XST and the positive drug Dl-3-n-butylphthalide (NBP) administered via intraperitoneal injection to observe vascular changes after stroke. The protective and pro-angiogenic effects of XST after stroke were demonstrated by Triphenyltetrazolium chloride staining and optical coherence tomography angiography. Subsequently, network pharmacology and molecular docking techniques, as well as *in vitro* experimental validation, were used to further analyze the potential mechanism by which XST promotes angiogenesis.

Results: The results showed that XST could reduce the cerebral infarction region in rats. And the neovascularization in the ischemic area of the rat brain significantly increased after 7 or 14 days of XST administration. Furthermore, XST could activate the vascular endothelial growth factor A (VEGFA)/vascular endothelial growth factor receptor 2 (VEGFR2), and hypoxia-inducible factor 1 (HIF-1) signaling pathways.

Conclusion: XST may promote post-stroke angiogenesis by affecting the HIF1-α/VEGFA/VEGFR2 signaling pathways.

1. Introduction

Cerebral stroke, which is a common cerebrovascular disease caused by a blockage in a blood vessel that prevents blood from flowing to the brain, or by a sudden rupture of a blood vessel in the brain that causes brain tissue damage, has become a leading cause of severe disability and death worldwide [1–3]. However, treatment of cerebral stroke is limited at present. The Food and Drug Administration has approved the

* Corresponding author. Beijing Key Laboratory of Innovative Drug Discovery of Traditional Chinese Medicine (Natural Medicine) and Translational Medicine, Institute of Medicinal Plant Development, Chinese Academy of Medical Sciences & Peking Union Medical College, Beijing, 100193, China
** Corresponding author. Xiyuan Hospital, China Academy of Chinese Medical Sciences, Beijing, 100193, China
*** Corresponding author. Beijing Key Laboratory of Innovative Drug Discovery of Traditional Chinese Medicine (Natural Medicine) and Translational Medicine, Institute of Medicinal Plant Development, Chinese Academy of Medical Sciences & Peking Union Medical College, Beijing, 100193, China.
E-mail addresses: lcao@implad.ac.cn (L. Cao), zxj6298@sohu.com (X. Zhang), sunguibo@126.com (G. Sun).

https://doi.org/10.1016/j.jgr.2024.08.004
Received 22 April 2023; Received in revised form 27 June 2024; Accepted 23 August 2024
Available online 27 August 2024

recombinant tissue plasminogen activator as the only verified treatment for cerebral stroke; however, it must be administered within 4.5 h of stroke for it to be effective [4,5]. Therefore, developing novel therapeutic methods to improve long-term rehabilitation after stroke remains challenging.

Angiogenesis refers to the physiological process by which new microvessels sprout from the pre-existing vasculature, including the proliferation and sprouting of endothelial cells, formation, branching, and anastomosis of tube-like vascular structures [6,7]. It is often stimulated by hypoxia and has been observed in the penumbra of the infarcted area of the brain in animal stroke models as well as in the brains of cerebral stroke patients [8]. Previous studies have reported that angiogenesis could reduce blood-brain barrier leakage and contribute to neuronal metabolism and remodeling [9,10]. Moreover, increased microvessel density in the peri-infarct region is closely correlated with prolonged survival in patients with cerebral stroke [11]. Therefore, promoting angiogenesis may be a promising therapeutic approach for cerebral stroke recovery.

Traditional Chinese Medicine (TCM) has been suggested as a potential remedy for cerebral infarction [12,13]. The Xueshuantong (XST) injection, a TCM preparation with Panax notoginseng saponins (PNS) as the predominant ingredient, is frequently prescribed in China for the treatment of cerebral infarction. PNS is the primary extract from the Chinese herbal medicine Panax notoginseng (Burkill) F.H.Chen [14]. Its main active ingredients include notoginsenoside R1, ginsenoside Rb1, ginsenoside Rd, ginsenoside Re, and ginsenoside Rg1 [15]. Numerous studies have shown that PNS protects the brain tissue from ischemia/reperfusion injury through anti-oxidative, anti-thrombotic, anti-inflammatory, neuroprotective, anti-apoptotic, and other properties [16–19]. However, it is unclear whether PNS can provide a protective effect in patients with ischemic stroke through angiogenesis and its possible mechanisms.

Thus, in this study, we observed vascular changes after stroke in rats using an *in vivo*, label-free, three-dimensional (3D) vascular imaging technique, optical coherence tomography angiography (OCTA), and aimed to demonstrate whether XST could promote vascular neovascularization in the ischemic region after stroke in rats. We also explored the potential mechanism of XST in promoting vascular neovascularization by utilizing network pharmacology and molecular docking techniques. Lastly, we experimentally validated whether XST promotes angiogenesis by affecting HIF1-α/VEGFA/VEGFR2 signaling pathways.

2. Materials and methods

2.1. Animals

Healthy Sprague-Dawley male rats (purchased from Charles River Institute, Beijing, China) weighing 250–280 g were selected for the experiments and kept in ventilated cages with a controlled temperature (20–25 °C), relative humidity (30–50 %), and a 12-h light/dark cycle with free access to food and water. The Institutional Animal Care and Use Committee's Guide for the Care and Use of the Chinese Academy of Medical Sciences and Peking Union Medical College was strictly followed for all animal experiments. Every attempt was made to use fewer animals and guarantee that they experienced the least amount of pain.

2.2. Middle cerebral artery occlusion/reperfusion surgery (MCAO/R)

Cerebral ischemia/reperfusion is caused by occlusion of the middle cerebral artery (MCAO/R), according to the procedure described by Meng et al. [20]. Prior to MCAO/R surgery, the rats received intraperitoneal doses of xylazine (10 mg/kg) and ketamine (80 mg/kg) to make them unconscious. To reduce bleeding after MCAO/R surgery, the wound was cleaned with iodine and stitched with sterile surgical sutures. An identical surgical approach was used for rats that underwent sham surgery, but the middle cerebral artery was not blocked. Throughout the treatment, a heating pad (Sunbeam, Boca Raton, FL, USA) was used to maintain the body temperature of the rats at 37 ± 0.5 °C.

2.3. Chemicals and drug administration

XST injection (Lyophilized; Cat. 20030315), mainly include notoginsenoside R1 (12.0 %, PubChem CID: 441934), ginsenoside Rg1 (43.6 %, PubChem CID: 441923), ginsenoside Re (5.9 %, PubChem CID: 441921), ginsenoside Rb1 (28.7 %, PubChem CID: 9898279), ginsenoside Rd (3.02 %, PubChem CID: 24721561) Supplementary Fig1 showed the HPLC chromatographic fingerprint analysis report of XST) was purchased from Guangxi Wuzhou Pharmaceuticals (GROUP) Co., Ltd. (Guangxi, China), and Dl-3-n-butylphthalide (NBP, Cat. 1182206134) was purchased from CSPC NBP Pharmaceutical Co., Ltd. (Shijiazhuang, China). XST was dissolved in 0.9 % saline and injected intraperitoneally. Following MCAO/R surgery, XST (25 mg/kg or 50 mg/kg), NBP (5 mg/kg), or the same amount of normal saline was administered to the rats. These medications were subsequently administered daily for 7 and 14 days, respectively, to assess angiogenesis. To better understand the mechanism of ischemic stroke modification in rats with MCAO/R by XST, brain tissues were collected at the end of the XST and NBP administration periods.

2.4. Evaluation of neurological deficits

The neurobehavioral evaluation was conducted on control and drug-treated animals (n = 6/group/time point) at 1, 3, 5, 7, 9, 11, and 13 days after surgery. In this experiment, neurological deficits of rats were assessed at different time points according to the modified neurological severity score (mNSS), an internationally recognized standard for the evaluation of neurological deficits in rats after ischemic cerebral stroke [21]. The mNSS scoring method includes a motor test, evaluation of the loss of reflexes and abnormal movements, sensory test, and balance beam test. The total score is 18, with higher scores indicating the more severe neurological impairment.

2.5. Triphenyltetrazolium chloride (TTC) staining

Rats were anesthetized and sacrificed by decapitation to maintain their brain integrity. The brain was placed in a special brain slot after freezing and was generally cut into 5–6 slices, one at 2 mm intervals. The slices were stained with a 2 % TTC solution (Cat. G3005) and placed in a 37 °C incubator for 15 min in the dark. After staining, the healthy tissue was rose-red in color and the infarcted tissue was white without staining. Then, the specimens were removed and fixed in 4 % paraformaldehyde (Cat. 20220518) for 24 h, placed on a light-colored operating table, and photographed using a digital camera. The results were calculated and expressed as a percentage infarction area, according to the brain infarction size = (sum of the white infarction area in each section)/(sum of the area of brain slices in each section) × 100 %.

2.6. OCTA

OCTA uses the relative motion of red blood cells and surrounding tissues as an endogenous blood flow marker feature instead of conventional exogenous fluorescent markers, and combines the spatial scattering signal acquisition capability of optical coherence imaging technology and the motion recognition capability of dynamic optical scattering characteristics to distinguish dynamic blood flow regions from static surrounding tissues in a 3D space [22]. To better record the cortical vasculature using the OCTA imaging system, a light window was created in the head of the rat for long-term observation and stabilization of the cortical vasculature. The cranial window was usually created on the right parietal bone.

The rats were positioned prone on a stereotactic frame with the head stabilized after being intraperitoneally injected with ketamine (80 mg/kg) and xylazine (10 mg/kg). A 4 × 4 mm craniotomy was performed 1 mm laterally using a dental drill. A round piece of cranial bone was carefully removed with forceps and replaced with a 5-mm diameter round clear glass cover. Cyanoacrylate bone cement (NISSIN, Shanghai, China) was used to adhere a glass cover to the skull, creating a flat tissue surface of 3 × 3 mm that served as an imaging window for microscopic examination of the major cerebral vessels in the sensorimotor cortical region. Subsequently, optical coherence tomography blood flow imaging was used to tomographically and algorithmically reconstruct the vascular signal within the target region to form a 3D spatial vascular network to detect the relevant parameters of the microvasculature in the ischemic brain region of rats.

2.7. Screening of active compounds and targets of PNS

To more comprehensively collect and organize information on PNS and their targets, three web-based pharmacological databases were searched: (TCMSP (https://tcmsp-e.com/), ETCM database (http://www.tcmip.cn/ETCM/index.php/Home), and TCMID database (https://bidd.group/TCMID/). In addition, PubMed (https://pubmed.ncbi.nlm.nih.gov/) and China National Knowledge Infrastructure (https://www.cnki.net/) were searched for articles on PNS and information on the related targets of PNS. The data of PNS and their targets from the aforementioned databases were collated, and after merging and de-duplication, standardized gene names of PNS-related targets were obtained using the UniProt database (https://www.uniprot.org/).

2.8. Construction of angiogenesis-related genes

Three databases were used to retrieve data on angiogenesis-related disease targets, including the GeneCards database (http://www.genecards.org/), DrugBank database (https://go.drugbank.com/), and DisGeNET database (http://www.disgenet.org/), and they were searched using "angiogenesis" as a keyword. Then, using the Excel spreadsheet function, the target data from the three aforementioned databases were combined, and after merging and de-duplication, standardized gene names were obtained using the UniProt database. Next, the obtained angiogenesis-related targets were compared with PNS targets to obtain crossover targets of angiogenesis and PNS. Venn diagrams were constructed online using Figdraw (https://www.figdraw.com/static/index.html) for visualization. Then, the information of angiogenesis and PNS cross-targets was imported into the STRING 11.5 database (http://string-db.org; where organisms was set to "*Homo sapiens*" and the minimum required interaction score was set to ≥0.9) to construct a protein-protein interaction (PPI) network and download the relevant results. Finally, the aforementioned results were visualized using the Cytoscape 3.9.1 software (https://www.cytoscape.org/), and the relevant information parameters were analyzed.

2.9. Gene ontology (GO) and kyoto encyclopedia of genes and genomes (KEGG) enrichment analysis

For the cross-targets of angiogenesis and PNS obtained in subsection 2.8, enrichment analysis was performed using GO and the KEGG with the DAVID database (https://david.ncifcrf.gov/), false discover rated <0.05 and P-value <0.05. Bubble and chord plots were used to visualize the first 30 GO items and KEGG pathways, respectively. Finally, Cytoscape 3.9.1 software (ClueGO plug-in) was used to conduct the enrichment network analysis.

2.10. Molecular docking

Five quality control components were screened from the PNS and docked to eight core target proteins. MGLTools 1.5.7 (https://ccsb.scripps.edu/mgltools/downloads/) and PyMOL 1.7.2.1 (https://pymol.org/2/) were used for molecular docking and visual analysis. High-resolution (Å< 2.50) protein 3D structure data of core targets were downloaded from the PDB database (https://www.rcsb.org/) and UniProt database (http://www.uniprot.org/). Next, the screened PNS and target information were entered into Auto Dock Vina (Screens Research Institute, Molecular Biology, CA, USA) software for molecular docking.

2.11. Western blot analysis

Western blot analysis was performed as previously reported [20]. The right cortical tissue from each rat (n = 3) was homogenized in a lysis buffer (P0013C; Beyotime, Nanjing, China) spiked with a protease (lot 01392/07821, ComWin Biotech, Beijing, China) and phosphatase inhibitor cocktail (lot 01385/12721, ComWin Biotech, Beijing, China), and the supernatant was collected by centrifugation and measured using BCA kit (Cat. CW0014S, ComWin Biotech, Beijing, China) to determine the total protein concentration. SDS-polyacrylamide gel electrophoresis was used to separate equal amounts of protein, which was then denatured with loading buffer and transferred to a membrane. After being blocked with 5 % milk, the membranes were incubated with the appropriate primary antibodies against the following proteins overnight at 4 °C: VEGFA (Proteintech, 19003-1-AP, 1:1000), VEGFR2 (Proteintech, 26415-1-AP, 1:1000), HIF1-α (ABclonal, A17906, 1:1000), AKT (ABclonal, A17909, 1:1000), p-AKT (ABclonal, AP0637, 1:1000) and β-actin (ABclonal, AC006, 1:1000). After three rinses, the membranes were treated with the required secondary antibodies. The blots were observed utilizing an enhanced chemiluminescence Western blot detection kit (Cat. CW00495) provided by ComWin Biotech. Blot density was measured using ImageJ software (National Institutes of health, Bethesda, MD, USA).

2.12. Statistical analysis

The data are presented as mean ± standard deviation and were gathered from three separate studies. If the data were normally distributed, one-way analysis of variance (ANOVA) followed by the Tukey test or two-way ANOVA followed by the Bonferroni multiple comparison test was performed. In cases where the data were not normally distributed, the Kruskal-Wallis test was used. SPSS (IBM Corp., Armonk, NY, USA) and GraphPad Prism 8.0 (GraphPad Software Inc., San Diego, CA, USA) were used to perform the statistical analysis. Statistical significance was set at $P < 0.05$.

3. Results

3.1. XST affects neurological function and body weight in rats with MCAO/R

We established a rat cerebral ischemia-reperfusion model using the MCAO/R method and assessed the success of the rat cerebral ischemia model using the mNSS. As shown in Fig. 1A, rats were administered the drug for 7 and 14 days after surgery, and body weight and mNSSs were recorded every other day during the administration period. The results showed that the body weight of rats gradually plateaued and tended to increase with the prolongation of XST and NBP administration (Fig. 1B (a), Fig. 1C(a)). The neurological function scores showed a decreasing trend, and the scores in the XST and NBP administration groups were lower than those in the MCAO/R group (Fig. 1B(b), Fig. 1C(b)).

3.2. XST attenuates MCAO/R-induced infarction volumes

To evaluate the neuroprotective effect of XST on MCAO/R injury, we examined cerebral infarction in the cortical and subcortical regions using TTC staining (Fig. 1D–F). The infarction volume was significantly increased in the MCAO/R group compared to the sham group, indicating

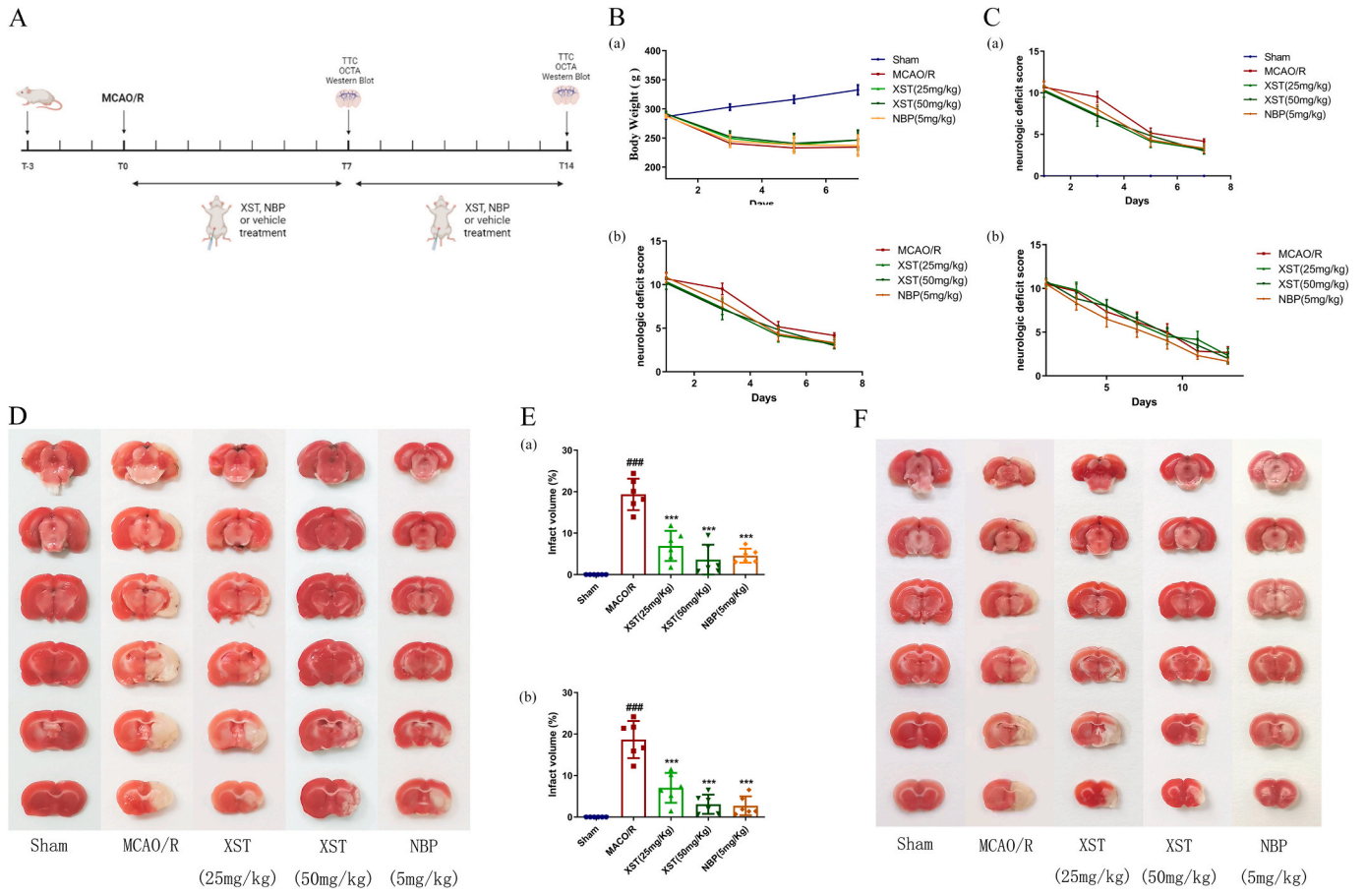

Fig. 1. XST treatment affected neurological function and body weight, reduced the infarct volume in MCAO/R rats. (A) The experimental design and sampling timeline. SD rats were subjected to MCAO/R and injected with 25 or 50 mg/kg XST, 5 mg/kg NBP or vehicle initially at 5 h post MCAO (3 h post reperfusion) and daily i.p. thereafter. (B) Weight (a) and neurological deficit scores (b) for a 7-day administration schedule. n = 6 per group. (C) Weight (a) and neurological deficit scores (b) for a 14-day administration schedule. n = 6. (D,F) TTC staining of brain sections from vehicle- or XST-treated and NBP-treated rats collected 7 or 14 days after stroke. (E) Effect of different concentrations of XST on infarct volume in rats after 7 days (a) or 14days (b) poststroke. Mean ± SD. n = 6 per group. $^{###}P < 0.001$ vs. sham group; $^{***}P < 0.001$ vs. MCAO/R group.

that the ischemia-reperfusion model was successfully constructed. The infarct volume was significantly reduced on days 7 and 14 rats treated with XST and NBP compared to the model group, suggesting that XST significantly suppressed ischemia-reperfusion injury in rats.

3.3. XST promotes post-ischemic angiogenesis

OCTA technology provides for *in vivo*, label-free, 3D flow movement angiography, which permits quick capture of information on blood perfusion in the capillary horizontal direction and allows for *in vivo* monitoring and assessment of blood perfusion and brain tissue damage. On days 7 and 14, awake rats are depicted in Fig. 2 with high-resolution vascular mapping and perfusion kinetics. On days 7 and 14, orthogonal projections of the 3D vessels in the ischemic area of the rat brain are shown in Fig. 2A and B. The XST and NBP administration in cerebrally ischemic rats greatly increased the number of tiny vessels in the wounded region. The vascular area density (Vad), vascular complexity index (Vci), vascular diameter index (Vdi), and vascular skeletal density (Vsd) were obtained using the VesQuant analysis software to analyze the angiograms for various perfusion kinetic indices.

According to the analysis, the Vad, Vci, Vdi, Vsd, and vascular perimeter index (Vpi) of the MCAO/R group on postoperative day 7 did not significantly differ from those in the sham group. In contrast, the Vad (Fig. 2A(a)), Vci (Fig. 2A(b)), Vpi (Fig. 2A(d)), and Vsd (Fig. 2A(e)) in the XST or NBP treatment group were significantly higher than those in the MCAO/R group. As shown in Fig. 2B, the Vad and Vsd were significantly higher on the postoperative day 14 in the MCAO/R group than in the sham group. The Vad (Fig. 2B(a)), Vci (Fig. 2B(b)), Vpi (Fig. 2B(d)), and Vsd (Fig. 2B(e)) in the ischemic region of the rats were significantly higher in the group that received XST or NBP administration than in the MCAO/R group after 14 days. These results indicate that XST can significantly promote vascular neovascularization in the ischemic injury region of rats and improve cerebral microcirculation after ischemia-reperfusion.

3.4. Prediction of the pathways of XST for promoting angiogenesis

The TCMSP, TCMID, and ETCM databases were searched, and 73 PNS components were obtained. To correct and standardize the retrieved gene names, the obtained target information was reviewed, merged, and de-duplicated before entering it into the UniProt database, yielding 487 potential target genes for PNS components (Supplementary Fig. 2A-E). The angiogenesis-related genes were then searched in the GeneCards, DisGeNET, and DrugBank databases. Duplicate genes were examined and eliminated, and finally, angiogenesis-related targets were screened. As a result of normalizing the gene names and entering the target information into the UniProt database, 5098 target genes associated with angiogenesis were identified.

Next, the target genes of the PNS components and angiogenesis-related target genes were used to create Venn diagrams, and 358 common targets (key targets) were discovered (Fig. 4 A). The PPI network diagram with 358 common targets had 23 nodes and 99 edges (Fig. 3).

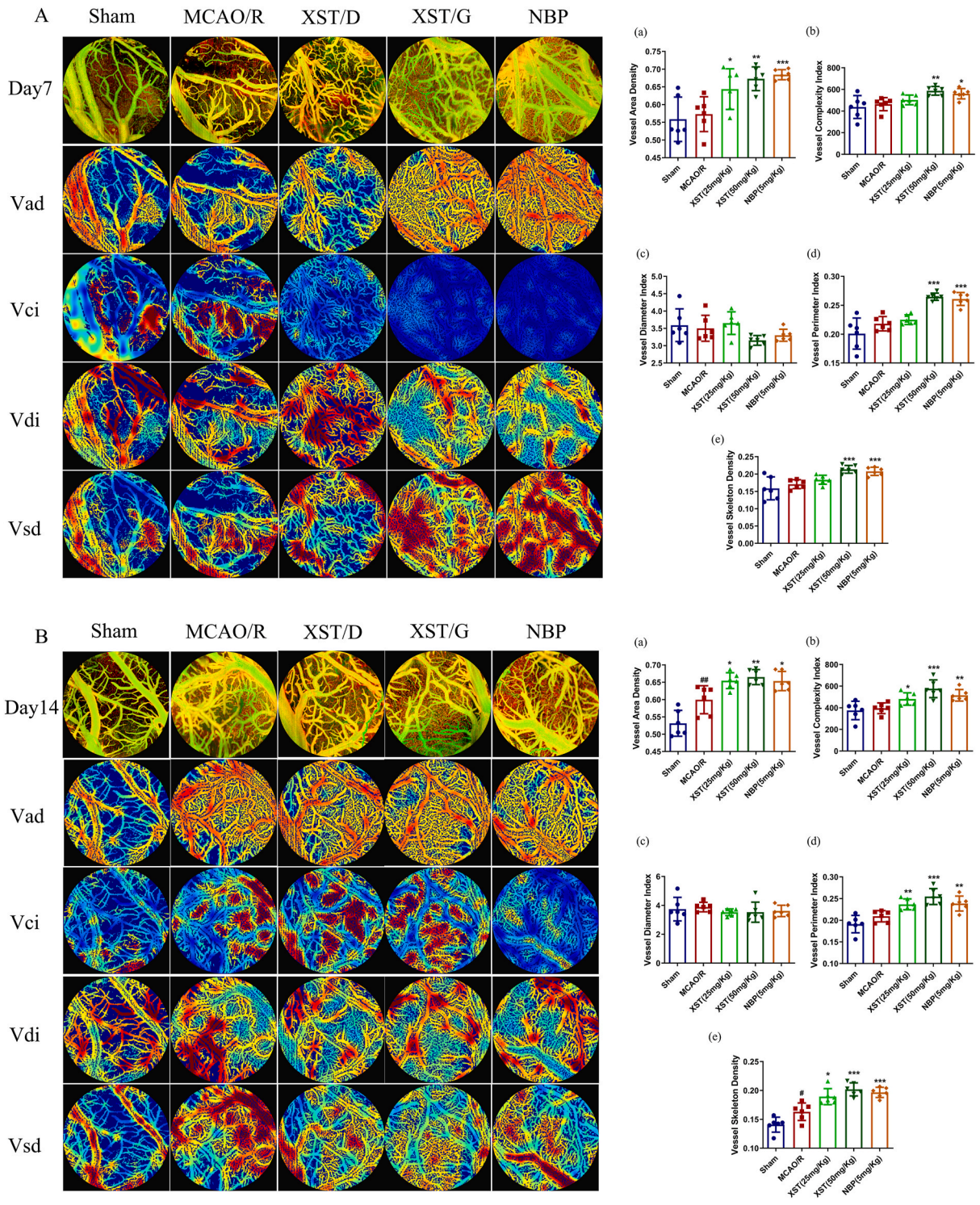

Fig. 2. XST treatment for 7, 14 days promoted post-stroke angiogenesis. (A, B) Imaging of blood vessels in the ischemic region of the brain acquired in the awake rats during resting state on Day 7, 14 after the cranial window surgery. And the Vad image, Vci image, Vdi image, and Vsd image obtained from VesQuant analysis software. Quantitative analysis of vascular network (Vad (a), Vci (b), Vdi (c), Vpi (d), and Vsd (e)) after XST or NBP treatment, n = 6 brains per group. Mean ± SD, $^{\#}P < 0.05$ and $^{\#\#}P < 0.01$ vs. sham group; $^{*}P < 0.05$, $^{**}P < 0.01$ and $^{***}P < 0.001$ vs. MCAO/R group.

The top 30 core genes of the PPI network graph according to the Closeness method were AKT1, GAPDH, EGFR, IL6, HSP90AA1, NFKB1, PTEN, MTOR, MAPK14, STAT3, ESR1, TNF, HRAS, NOS3, AGT, MAPK1, MAPK8, CCND1, BCL2L1, MAPK3, PPARG, VEGFA, PIK3CA, TGFB1, CREBBP, MMP9, IGF1, LEP, EDN1, CDK2.

Then, the DAVID online tool was used to perform gene function and pathway enrichment analyses of the key targets, and 2234 GO entries were obtained and were significantly enriched ($P < 0.05$). The analyses included 1833 biological processes, such as cellular responses to oxygenated compounds; 118 cellular components, such as cytoplasm and intracellular vesicles; and 283 molecular functions, such as protein kinase activity and phosphate transferase activity. The top-ranked and directly regulated pathways of angiogenesis, including the PI3K-AKT pathway, VEGF pathway, and HIF-1 pathway, involving the targets

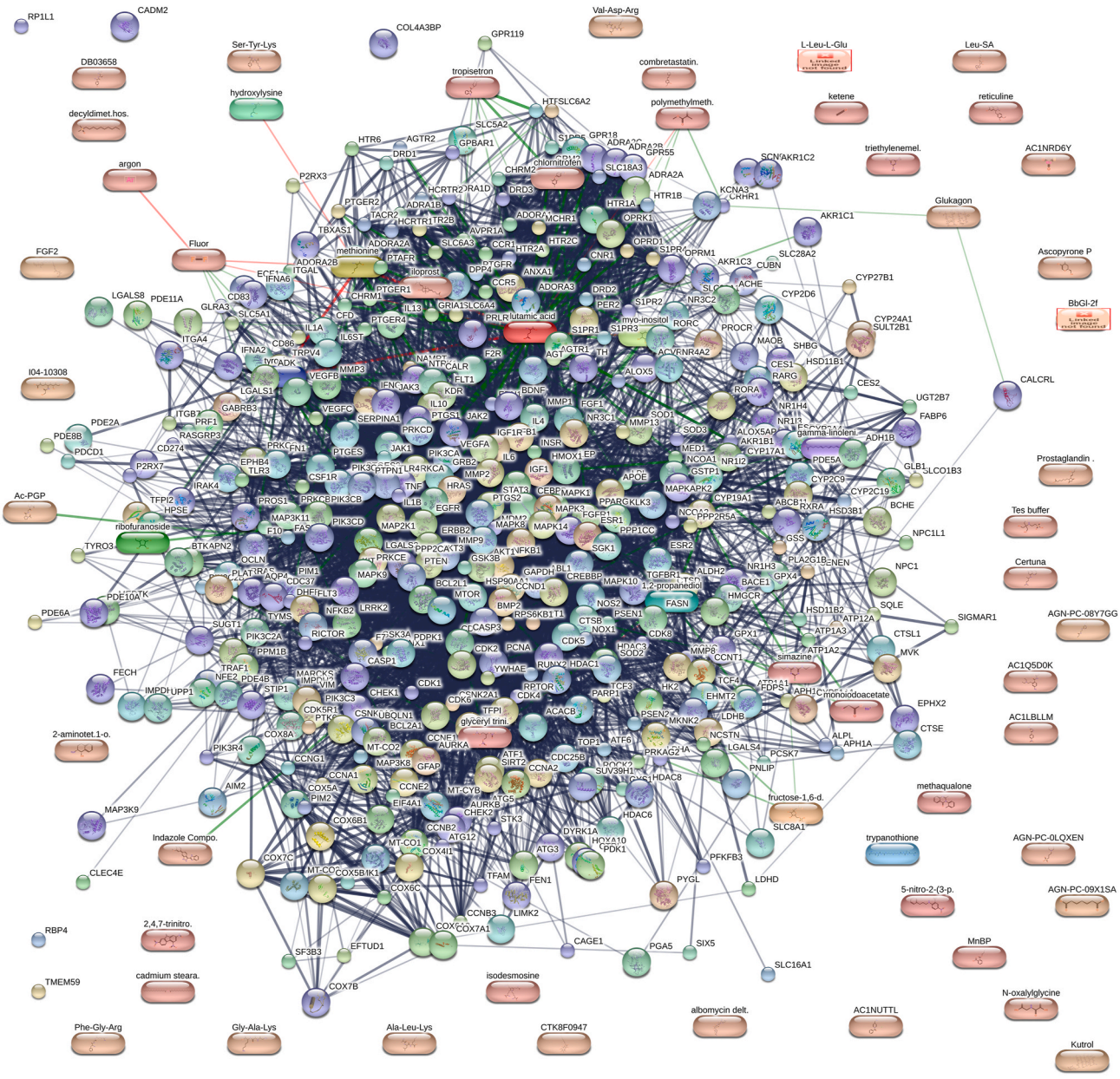

Fig. 3. PPI network of 358 common targets.

AKT1, GAPDH, EGFR, IL6, HSP90AA1, NFKB1, PTEN, MTOR, MAPK14, STAT3, NOS3, VEGFA, CDK2, and others, were among the 139 KEGG entries that were obtained (Fig. 4B–C). The width of the nodes in the chord diagram represents the magnitude of the association between targets in the pathway; the smaller the P value, the wider the width.

3.5. Prediction of the targets of XST for promoting angiogenesis

The molecular docking technique was used to verify the binding of the primary pharmacodynamic components of PNS (notoginsenoside R1, ginsenoside Rb1, ginsenoside Rd, ginsenoside Re, and ginsenoside Rg1) and the positive drug NBP to key targets (VEGFA, VEGFR2, HIF1-α, and AKT1) (Fig. 5A–D). The primary pharmacodynamic components of PNS had a stronger affinity for the core targets than the positive drug NBP in the best mode (Fig. 4D).

3.6. XST promotes angiogenesis by activating the VEGFA/VEGFR2 and HIF1-α pathways

To determine whether XST promotes angiogenesis through these core targets, the protein expression levels of VEGFA/VEGFR2, p-AKT/AKT, and HIF1-α were assessed by Western blot. As shown in Fig. 6, the expression level of VEGFR2 was significantly decreased while the expression levels of p-AKT, AKT, and HIF1-α were significantly increased in the MCAO/R group compared to the sham group. Both XST and NBP significantly increased the expression levels of VEGFA, VEGFR2, AKT, P-AKT, and HIF1-α in the infarct region of the brain on day 14 compared to MCAO/R. Among them, XST had a stronger effect on VEGFR2 activation than the positive drug NBP. This result suggested that XST performed a role in promoting post-stroke angiogenesis through the HIF1-α/VEGFA/VEGFR2 pathways.

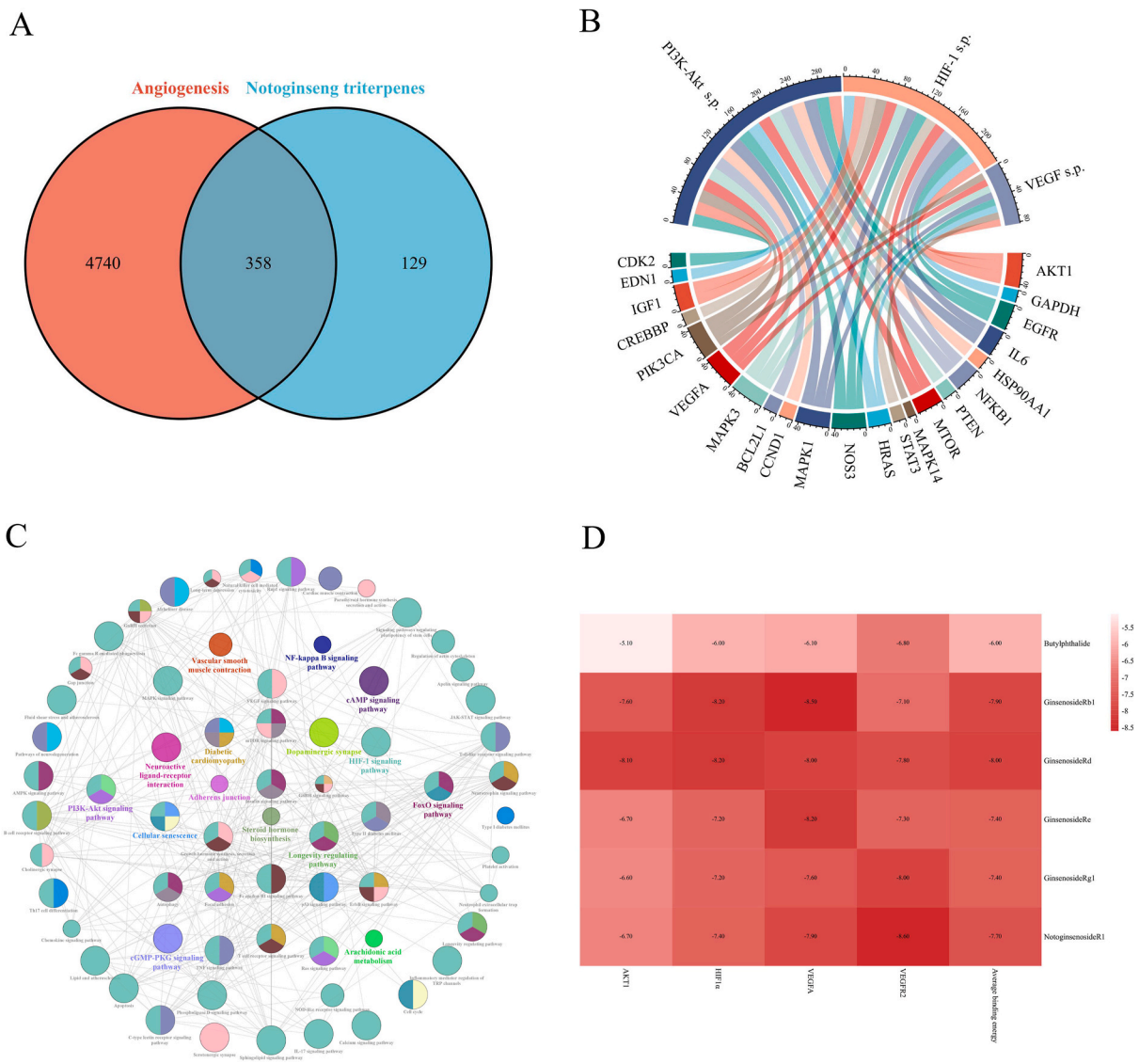

Fig. 4. Prediction of the pathways and targets of XST for promoting angiogenesis. (A) The Venn diagrams of the target genes of PNS components and angiogenesis-related target genes. (B, C) The chord diagram and network of the top 30 KEGG pathways. Chords, the relationship between pathways and targets; width and scale, degree of correlation. S.P. means signing pathway. (D) Molecular docking heatmap of main components and key targets (Kcal/mol).

4. Discussion

Stroke is a leading cause of mortality and disability in adults worldwide, with the highest number fatalities occurring in China [23]. Post-stroke vascularization is a key treatment for ischemic stroke and has great therapeutic potential [24,25]. The efficiency of XST in stimulating blood circulation and dissipating blood stasis has made it a common treatment option in clinical practice [26]. Previous studies have reported that XST may provide long-term neuroprotection in rats with MCAO/R by affecting the Nrf2-VEGF or JAK2/STAT3 pathways, but little has been reported about the role of XST in post-stroke vascularization [14,15]. In our study, we demonstrated for the first time through OCTA that XST has the potential to significantly improve vascular neovascularization and microcirculation in rats with cerebral ischemia and reperfusion. The advancement of ischemic stroke revascularization may be attributed to the activation of VEGFA/VEGFR2, HIF1-α, and PI3K/AKT pathways by XST.

After the ischemic semidark zone tissue is deprived of oxygen and nutrients due to stroke, angiogenic factors would be released and caused endothelial cell and endothelial progenitor cell proliferation, resulting in the formation of new blood vessels [27]. This process, known as angiogenesis, facilitates the restoration of oxygen and nutrient supply to ischemic brain tissue. Boosting the growth of blood vessels to restore the blood supply to the brain's microvasculature can improve brain circulation and preserve neurons, allowing for brain plasticity and recovery of neurological function [28]. Therefore, neovascularization is a viable treatment option for patients with stroke. Evidence from past research suggests that specific components of PNS, such as notoginsenoside R1, could potentially enhance the survival rate of rats that have suffered a stroke through the formation of new blood vessels [29]. Studies have indicated that stroke-induced revascularization occurs 3–4 days after the initial ischemic injury and persists for >21 days [30,31]. Research on cerebral ischemic rat has shown an initial gradual decrease in the number of main and peripheral small vessels in the ischemic region, followed by compensatory thickening of the collateral vessels, which ultimately return to their original vessel diameters, as well as a significant increase in the number of small vessels [32]. In addition, a positive correlation was observed between microvessel density and survival in patients who had suffered from stroke and survived for a few days or weeks [11].

OCTA is a non-invasive, label-free optical imaging technique that resolves the microscopic architecture of living biological tissues within a

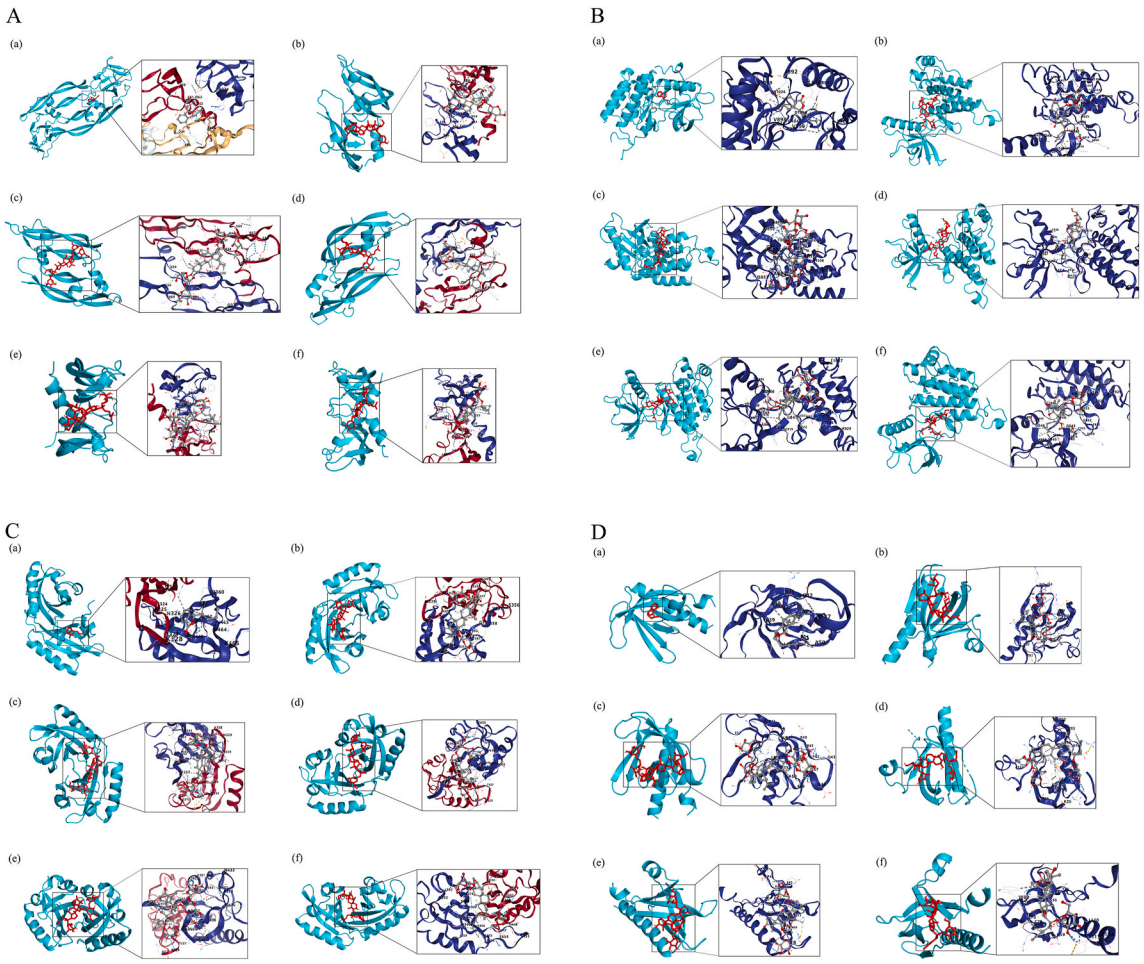

Fig. 5. 3D molecular docking diagrams of PNS active components and target, displaying the binding patterns of VEGFA (A), VEGFR2 (B), HIF1-α (C) and AKT1 (D) complex with NBP (a), notoginsenoside R1 (b), ginsenoside Rb1 (c), ginsenoside Rd (d), ginsenoside Re (e), and ginsenoside Rg1 (f). In each group of photographs, a perspective view is shown on the left and a close-up view of the specific docking position is shown on the right.

few millimeters of view, allowing for the acquisition of data on blood perfusion, blood flow velocity, and optical characteristics of perfused tissue [33]. Additionally, without the need for external contrast agents, OCTA improves the contrast of the movement of red blood cells flowing through the vessel lumen, enabling visualization of the complex vascular network and circulation in the rat cerebral cortex [34]. In an earlier study, OCTA was used to examine the vascularity and blood flow of the cortical tissue in a rat model of ischemic stroke [35]. In our study, we used OCTA technology to provide real-time imaging of cerebral ischemia regions in rats 7 and 14 days after stroke to record the changes in vascularity induced by MCAO/R and drug administration in the ischemic areas of the brain. Consistent with the findings of earlier reports, our study showed that the MCAO/R model group had more microvessels than the healthy group, especially on day 14, and had a significantly higher vascular area density and vascular skeleton density. In addition, the Vad, Vci, Vpi, and Vsd were all significantly higher within 1 or 2 weeks in the XST and NBP groups than in the healthy and MCAO/R model groups. As a result, we conclude that XST can ameliorate brain injuries caused by cerebral ischemia-reperfusion in rats, promote vascular neovascularization in the ischemic area after stroke, and improve the survival rate after stroke.

Considering the complicated mechanism of PNS, network pharmacology and molecular docking techniques were used to explore the pro-angiogenic targets of XST in this study. Our analysis of various network pharmacology databases showed that PNS contained approximately 73 bioactive ingredients, which corresponded to 487 potential target genes, of which 358 overlapped with the range of target genes associated with angiogenesis. The PPI results indicated that AKT1, NFKB1, STAT3, VEGFA, PIK3CA, and other molecules were the key targets of PNS in promoting angiogenesis. These key targets involved 283 molecular functions, 118 cellular components, and 1833 biological processes. Among them, the PI3K-AKT, VEGF, and HIF-1 signaling pathways are highly ranked and directly regulate angiogenesis. Several of these signaling pathways have been proven in previous studies to be associated with herbal-mediated angiogenesis. For example, ginsenoside Rg1, a bioactive component of ginseng, has been shown to facilitate brain regeneration by regulating angiogenesis and neurogenesis and by targeting HIF-1 [36]. Danshen injection has also been reported to enhance HIF-1 and VEGFA expressions, which, in turn, improve hypoxia-induced angiogenesis in mice [37]. Thus, we molecularly docked the positive drug NBP with VEGFA, VEGFR2, HIF-1, and AKT as well as the five index components of PNS. The results demonstrated that the primary pharmacological elements of PNS had a higher affinity for the key targets and the binding energy to all of these targets was higher than that of the positive drug in the best mode.

VEGF, a pro-angiogenic cytokine that is extensively expressed, is the most crucial element in controlling the process of angiogenesis among these targets. It contains placental growth factors, VEGFA, VEGFB, and VEGFC, among which VEGFA regulates and promotes angiogenesis in a range of pathological disorders [38–41]. In response to changes in intracellular oxygen levels, HIF-1 upregulates VEGFA in ischemic brain tissue to induce angiogenesis in ischemic stroke induced by hypoxia

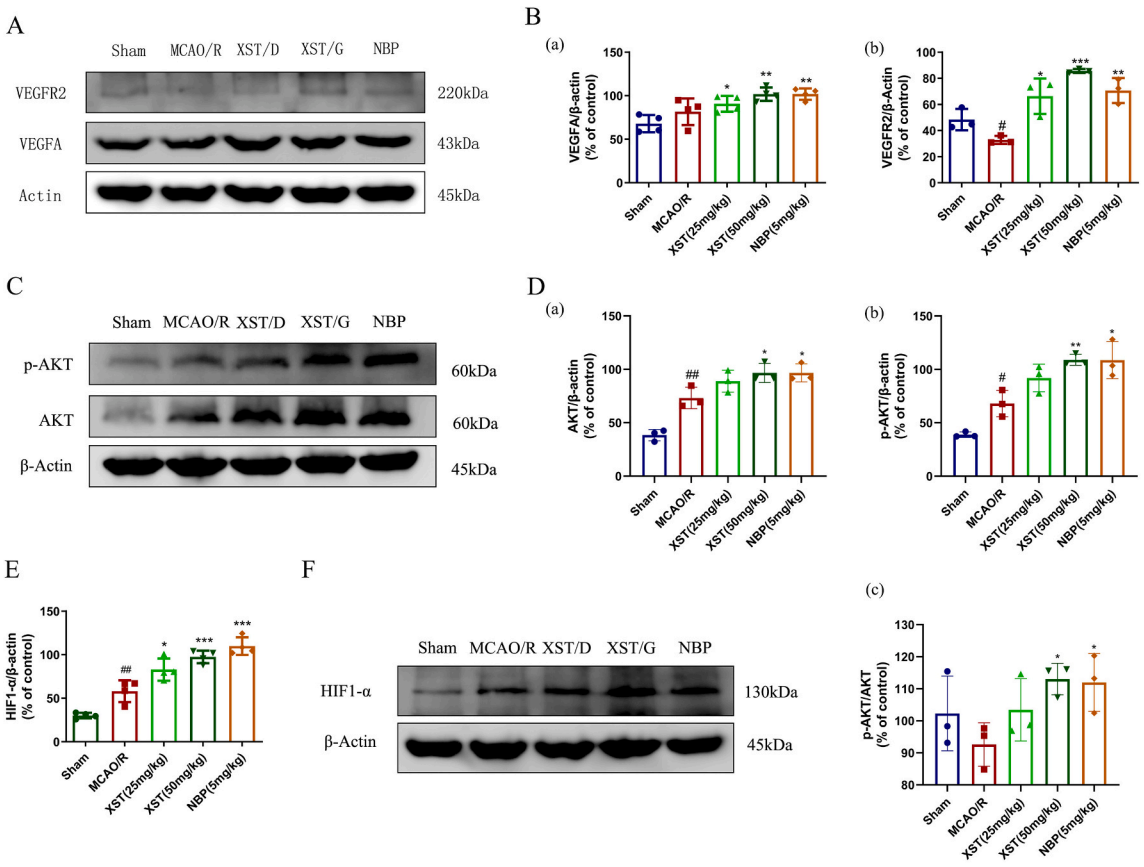

Fig. 6. XST promoted angiogenesis by activating VEGFA/VEGFR2 pathway, HIF1α pathway and PI3K/AKT pathway. Representative Western blot images (A, C, F) and quantification of relative protein levels of VEGFA (B(a)), VEGFR2 (B(b)), p-AKT (D(a)), AKT (D(b)), p-AKT/AKT (D(c)), HIF1-α (E) in the infarct region of the Sham, MCAO/R, XST and NBP groups on day 14 after MCAO/R operation, n = 3 in each group. Mean ± SD, $^{\#}P < 0.05$ and $^{\#\#}P < 0.01$ vs. sham group; $^{*}P < 0.05$, $^{**}P < 0.01$ and $^{***}P < 0.001$ vs. MCAO/R group. β-Actin was used as loading control.

[42]. Subsequently, VEGFA gene expression is upregulated, and the protein that is produced typically binds to VEGFR-2, leading to the induction of angiogenesis [43]. Additionally, various signaling pathways, such as the PI3K/AKT protein kinase pathway, facilitate VEGF-induced activities [44,45]. The PI3K/AKT signaling pathway is involved in numerous cellular processes, including cell proliferation, migration, spreading, and survival [46]. Neointima formation is significantly influenced by increased PI3K/AKT pathway activation [47,48]. In both HIF-1-dependent and HIF-1-independent manners, PI3K/AKT protein kinase pathway activation during normal vascular development can promote angiogenesis [49,50]. It has been previously reported that ginsenoside Rg1 was able to act as a potent regulator of HIF-1, and Notoginsenoside Ft1 was able to promote HIF1-α nuclear translocation, which induced the binding of HIF1-α to the VEGF promoter [51,52]. And our study found that XST was able to significantly activate HIF1-α, increase VEGFA and VEGFR2 levels, and significantly enhance p-AKT and AKT activities. Therefore, XST may facilitate post-stroke ischemic region revascularization by affecting the HIF1-α/VEGFA/VEGFR2 and signaling pathways.

5. Conclusion

Herein, vascular changes in the post-stroke ischemic region were first observed *in vivo* using the OCTA technique, demonstrating the promoting effect of XST on vascular neovascularization in the ischemic region. Additionally, the potential mechanism by which XST promotes vascular neovascularization was systematically investigated and validated from various perspectives using network pharmacology and molecular docking methods. Finally, the results of the experimental validation demonstrated that XST might stimulate the HIF1-α/VEGFA/VEGFR2 and signaling pathways, hence promoting post-stroke ischemic region revascularization. This serves as a framework for the subsequent investigation for the impact of PNS on angiogenesis.

Founding

This work was supported by the CAMS Innovation Fund for Medical Sciences (CIFMS), 2021-I2M-1–031, National Key Research and Development Program of China, No.2023YFD2201802 and Yunnan Province Science and Technology Department (No.202102AA310048).

Data available statement

The raw data supporting the conclusions of this article will be made available by the authors, without undue reservation.

Ethics statement

All animal care and experimental procedures were reported in accordance with the Institutional Animal Care and Use Committee's Guide for the Care and Use of the Chinese Academy of Medical Sciences and Peking Union Medical College.

Abbreviations: TCM, Traditional Chinese medicine; XST, Xueshuantong; NBP, Dl-3-n-butylphthalide; PNS, *Panax notoginseng saponins*; 3D, three-dimensional; OCTA, optical coherence tomography angiography; VEGFA, vascular endothelial growth factor A; VEGFR2, vascular endothelial growth factor receptor 2; HIF-1, hypoxia-inducible factor 1; PI3K, phosphatidylinositol 3-kinase; MCAO/R, middle cerebral

artery occlusion/reperfusion; mNSS, modified neurological severity score; TTC, Triphenyltetrazolium chloride; Vad, vascular area density; Vci, vascular complexity index; Vdi, vascular diameter index; Vsd, vascular skeletal density; Vpi, vascular perimeter index.

CRediT authorship contribution statement

Haiyan Xiao: and, with contributions from. **Shusen Liu:** and. **Binyu Fang:** and. **Wenchao Zhang:** performed and analyzed experiments. **Min Wang:** and. **Jingxue Ye:** and. **Tianxiao Huang:** performed data analysis and statistical processing. **Li Cao:** conceived the whole experiment. The paper was written by, All authors reviewed the manuscript and agree to be accountable for all aspects of work ensuring integrity and accuracy. **Xiaojun Zhang:** and. **Guibo Sun:** and, and.

Declaration of competing interest

The authors declare that the research was conducted in the absence of any commercial or financial relationships that could be construed as a potential conflict of interest.

Appendix A. Supplementary data

Supplementary data related to this article can be found at https://doi.org/10.1016/j.jgr.2024.08.004.

References

[1] Donnan GA, Fisher M, Macleod M, Davis SM. Stroke. Lancet. 2008;371(9624):1612–23.
[2] Feske SK. Ischemic stroke. Am J Med 2021;134(12):1457–64.
[3] Wu S, Wu B, Liu M, Chen Z, Wang W, Anderson CS, et al. Stroke in China: advances and challenges in epidemiology, prevention, and management. Lancet Neurol 2019;18(4):394–405.
[4] Kirmani JF, Alkawi A, Panezai S, Gizzi M. Advances in thrombolytics for treatment of acute ischemic stroke. Neurology 2012;79(13 Suppl 1):S119–25.
[5] Lekoubou A, Awoumou JJ, Kengne AP. Incidence of seizure in stroke patients treated with recombinant tissue plasminogen activator: a systematic review and meta-analysis. Int J Stroke 2017;12(9):923–31.
[6] Madelaine R, Sloan SA, Huber N, Notwell JH, Leung LC, Skariah G, et al. MicroRNA-9 couples brain neurogenesis and angiogenesis. Cell Rep 2017;20(7):1533–42.
[7] Kanazawa M, Takahashi T, Ishikawa M, Onodera O, Shimohata T, Del Zoppo GJ. Angiogenesis in the ischemic core: a potential treatment target? J Cereb Blood Flow Metab 2019;39(5):753–69.
[8] Li H, Liao Y, Gao L, Zhuang T, Huang Z, Zhu H, et al. Coronary serum exosomes derived from patients with myocardial ischemia regulate angiogenesis through the miR-939-mediated nitric oxide signaling pathway. Theranostics 2018;8(8):2079–93.
[9] Hatakeyama M, Ninomiya I, Kanazawa M. Angiogenesis and neuronal remodeling after ischemic stroke. Neural Regen Res 2020;15(1):16–9.
[10] Fang J, Wang Z, Miao CY. Angiogenesis after ischemic stroke. Acta Pharmacol Sin 2023;44(7):1305–21.
[11] Krupinski J, Kaluza J, Kumar P, Kumar S, Wang JM. Role of angiogenesis in patients with cerebral ischemic stroke. Stroke 1994;25(9):1794–8.
[12] Li XH, Yin FT, Zhou XH, Zhang AH, Sun H, Yan GL, et al. The signaling pathways and targets of natural compounds from traditional Chinese medicine in treating ischemic stroke. Molecules 2022;27(10).
[13] Bangar A, Khan H, Kaur A, Dua K, Singh TG. Understanding mechanistic aspect of the therapeutic role of herbal agents on neuroplasticity in cerebral ischemic-reperfusion injury. J Ethnopharmacol 2024;319(Pt 2):117153.
[14] Guo H, Adah D, James PB, Liu Q, Li G, Ahmadu P, et al. Xueshuantong injection (lyophilized) attenuates cerebral ischemia/reperfusion injury by the activation of nrf2-VEGF pathway. Neurochem Res 2018;43(5):1096–103.
[15] Wang G, Chen Z, Song Y, Wu H, Chen M, Lai S, et al. Xueshuantong injection alleviates cerebral microcirculation disorder in middle cerebral artery occlusion/reperfusion rats by suppressing inflammation via JNK mediated JAK2/STAT3 and NF-κB signaling pathways. J Ethnopharmacol 2022;298:115592.
[16] Shi X, Yu W, Liu L, Liu W, Zhang X, Yang T, et al. Panax notoginseng saponins administration modulates pro-/anti-inflammatory factor expression and improves neurologic outcome following permanent MCAO in rats. Metab Brain Dis 2017;32(1):221–33.
[17] Hu S, Wu Y, Zhao B, Hu H, Zhu B, Sun Z, et al. Panax notoginseng saponins protect cerebral microvascular endothelial cells against oxygen-glucose deprivation/reperfusion-induced barrier dysfunction via activation of PI3K/Akt/Nrf2 antioxidant signaling pathway. Molecules 2018;23(11).
[18] Wu Y, Wang W, Kou N, Wang M, Yang L, Miao Y, et al. Panax notoginseng saponins combined with dual antiplatelet drugs potentiates anti-thrombotic effect with alleviated gastric injury in A carotid artery thrombosis rat model. J Stroke Cerebrovasc Dis 2022;31(8):106597.
[19] Zhou D, Cen K, Liu W, Liu F, Liu R, Sun Y, et al. Xuesaitong exerts long-term neuroprotection for stroke recovery by inhibiting the ROCKII pathway, in vitro and in vivo. J Ethnopharmacol 2021;272:113943.
[20] Meng X, Wang M, Wang X, Sun G, Ye J, Xu H, et al. Suppression of NADPH oxidase- and mitochondrion-derived superoxide by Notoginsenoside R1 protects against cerebral ischemia-reperfusion injury through estrogen receptor-dependent activation of Akt/Nrf2 pathways. Free Radic Res 2014;48(7):823–38.
[21] Chen J, Sanberg PR, Li Y, Wang L, Lu M, Willing AE, et al. Intravenous administration of human umbilical cord blood reduces behavioral deficits after stroke in rats. Stroke 2001;32(11):2682–8.
[22] Wang L, Chen Z, Li Y, Yang J, Li Y. Optical coherence tomography angiography for noninvasive evaluation of angiogenesis in a limb ischemia mouse model. Sci Rep 2019;9(1):5980.
[23] Feigin VL, Norrving B, Mensah GA. Global burden of stroke. Circ Res 2017;120(3):439–48.
[24] Zong X, Li Y, Liu C, Qi W, Han D, Tucker L, et al. Theta-burst transcranial magnetic stimulation promotes stroke recovery by vascular protection and neovascularization. Theranostics 2020;10(26):12090–110.
[25] Kolbinger A, Kestner RI, Jencio L, Schäufele TJ, Vutukuri R, Pfeilschifter W, et al. Behind the wall-compartment-specific neovascularisation during post-stroke recovery in mice. Cells 2022;11(10).
[26] Bu L, Dai O, Zhou F, Liu F, Chen JF, Peng C, et al. Traditional Chinese medicine formulas, extracts, and compounds promote angiogenesis. Biomed Pharmacother 2020;132:110855.
[27] Hermann DM, Zechariah A. Implications of vascular endothelial growth factor for postischemic neurovascular remodeling. J Cereb Blood Flow Metab 2009;29(10):1620–43.
[28] Yang Y, Torbey MT. Angiogenesis and blood-brain barrier permeability in vascular remodeling after stroke. Curr Neuropharmacol 2020;18(12):1250–65.
[29] Zhu T, Xie WJ, Wang L, Jin XB, Meng XB, Sun GB, et al. Notoginsenoside R1 activates the NAMPT-NAD(+)-SIRT1 cascade to promote postischemic angiogenesis by modulating Notch signaling. Biomed Pharmacother 2021;140:111693.
[30] Yu SW, Friedman B, Cheng Q, Lyden PD. Stroke-evoked angiogenesis results in a transient population of microvessels. J Cereb Blood Flow Metab 2007;27(4):755–63.
[31] Tregub PP, Averchuk AS, Baranich TI, Ryazanova MV, Salmina AB. Physiological and pathological remodeling of cerebral microvessels. Int J Mol Sci 2022;23(20).
[32] Krupinski J, Stroemer P, Slevin M, Marti E, Kumar P, Rubio F. Three-dimensional structure and survival of newly formed blood vessels after focal cerebral ischemia. Neuroreport 2003;14(8):1171–6.
[33] Choi WJ, Reif R, Yousefi S, Wang RK. Improved microcirculation imaging of human skin in vivo using optical microangiography with a correlation mapping mask. J Biomed Opt 2014;19(3):36010.
[34] Wang RK, Jacques SL, Ma Z, Hurst S, Hanson SR, Gruber A. Three dimensional optical angiography. Opt Express 2007;15(7):4083–97.
[35] Dziennis S, Qin J, Shi L, Wang RK. Macro-to-micro cortical vascular imaging underlies regional differences in ischemic brain. Sci Rep 2015;5:10051.
[36] Chan LS, Yue PY, Wong YY, Wong RN. MicroRNA-15b contributes to ginsenoside-Rg1-induced angiogenesis through increased expression of VEGFR-2. Biochem Pharmacol 2013;86(3):392–400.
[37] Ai F, Chen M, Li W, Yang Y, Xu G, Gui F, et al. Danshen improves damaged cardiac angiogenesis and cardiac function induced by myocardial infarction by modulating HIF1α/VEGFA signaling pathway. Int J Clin Exp Med 2015;8(10):18311–8.
[38] Shibuya M. Vascular endothelial growth factor (VEGF) and its receptor (VEGFR) signaling in angiogenesis: a crucial target for anti- and pro-angiogenic therapies. Genes Cancer 2011;2(12):1097–105.
[39] Melincovici CS, Boşca AB, Şuşman S, Märginean M, Mihu C, Istrate M, et al. Vascular endothelial growth factor (VEGF) - key factor in normal and pathological angiogenesis. Rom J Morphol Embryol 2018;59(2):455–67.
[40] Shibuya M. Vascular endothelial growth factor and its receptor system: physiological functions in angiogenesis and pathological roles in various diseases. J Biochem 2013;153(1):13–9.
[41] Wang L, Chopp M, Gregg SR, Zhang RL, Teng H, Jiang A, et al. Neural progenitor cells treated with EPO induce angiogenesis through the production of VEGF. J Cereb Blood Flow Metab 2008;28(7):1361–8.
[42] Shweiki D, Itin A, Soffer D, Keshet E. Vascular endothelial growth factor induced by hypoxia may mediate hypoxia-initiated angiogenesis. Nature 1992;359(6398):843–5.
[43] Beck H, Plate KH. Angiogenesis after cerebral ischemia. Acta Neuropathol 2009;117(5):481–96.
[44] Polverini PJ. Angiogenesis in health and disease: insights into basic mechanisms and therapeutic opportunities. J Dent Educ 2002;66(8):962–75.
[45] Jiang BH, Zheng JZ, Aoki M, Vogt PK. Phosphatidylinositol 3-kinase signaling mediates angiogenesis and expression of vascular endothelial growth factor in endothelial cells. Proc Natl Acad Sci U S A 2000;97(4):1749–53.
[46] Azad AK, Zhabyeyev P, Vanhaesebroeck B, Eitzen G, Oudit GY, Moore RB, et al. Inactivation of endothelial cell phosphoinositide 3-kinase β inhibits tumor angiogenesis and tumor growth. Oncogene 2020;39(41):6480–92.
[47] Bader AG, Kang S, Zhao L, Vogt PK. Oncogenic PI3K deregulates transcription and translation. Nat Rev Cancer 2005;5(12):921–9.

[48] Shi G, Chen J, Zhang C, Zhao X, Wang J, Chen R, et al. Astragaloside IV promotes cerebral angiogenesis and neurological recovery after focal ischemic stroke in mice via activating PI3K/Akt/mTOR signaling pathway. Heliyon 2023;9(12):e22800.
[49] Karar J, Maity A. PI3K/AKT/mTOR pathway in angiogenesis. Front Mol Neurosci 2011;4:51.
[50] Jiang BH, Jiang G, Zheng JZ, Lu Z, Hunter T, Vogt PK. Phosphatidylinositol 3-kinase signaling controls levels of hypoxia-inducible factor 1. Cell Growth Differ 2001;12(7):363–9.
[51] Leung KW, Ng HM, Tang MK, Wong CC, Wong RN, Wong AS. Ginsenoside-Rg1 mediates a hypoxia-independent upregulation of hypoxia-inducible factor-1α to promote angiogenesis. Angiogenesis 2011;14(4):515–22.
[52] Shen K, Ji L, Gong C, Ma Y, Yang L, Fan Y, et al. Notoginsenoside Ft1 promotes angiogenesis via HIF-1α mediated VEGF secretion and the regulation of PI3K/AKT and Raf/MEK/ERK signaling pathways. Biochem Pharmacol 2012;84(6):784–92.